

## ION-COUNTING NANODOSEMETER WITH PARTICLE TRACKING CAPABILITIES

V. Bashkirov<sup>1,\*</sup>, R. Schulte<sup>1</sup>, A. Breskin<sup>2</sup>, R. Chechik<sup>2</sup>, S. Schemelinin<sup>2</sup>, G. Garty<sup>3</sup>,  
A. Wroe<sup>4</sup>, H. Sadrozinski<sup>5</sup> and B. Grosswendt<sup>6</sup>

<sup>1</sup>Loma Linda University Medical Center, 11175 Campus Street, Loma Linda,  
CA 92354, USA

<sup>2</sup>Weizmann Institute of Science, 76100 Rehovot, Israel

<sup>3</sup>Currently at RARAF, Columbia University, P.O. Box 21, Irvington, NY 10533, USA

<sup>4</sup>Centre for Medical Radiation Physics, University of Wollongong, Wollongong,  
NSW 2522, Australia

<sup>5</sup>Santa Cruz Institute of Particle Physics, 1156 High Street, Santa Cruz, CA 95064, USA

<sup>6</sup>Physikalisch-Technische Bundesanstalt, Bundesallee 100, 38116 Braunschweig,  
Germany

**An ion-counting nanodosimeter (ND) yielding the distribution of radiation-induced ions in a low-pressure gas within a millimetric, wall-less sensitive volume (SV) was equipped with a silicon microstrip telescope that tracks the primary particles, allowing correlation of nanodosimetric data with particle position relative to the SV. The performance of this tracking ND was tested with a broad 250 MeV proton beam at Loma Linda University Medical Center. The high-resolution tracking capability made it possible to map the ion registration efficiency distribution within the SV, for which only calculated data were available before. It was shown that tracking information combined with nanodosimetric data can map the ionisation pattern of track segments within 150 nm-equivalent long SVs with a longitudinal resolution of  $\sim 5$  tissue-equivalent nanometers. Data acquired in this work were compared with results of Monte Carlo track structure simulations. The good agreement between ‘tracking nanodosimetry’ data acquired with the new system and simulated data supports the application of ion-counting nanodosimetry in experimental track-structure studies.**

### INTRODUCTION

The spatial distribution of radiation interactions has long been recognised as an important factor for the induction and quality of DNA damage<sup>(1,2)</sup>. Therefore, significant effort has been invested into the development of numerical simulation codes modelling particle track structure on the nanometer scale<sup>(3,4)</sup>. In comparison, experimental investigations in this area are rather scarce but are important for verification of track model predictions.

One of a few existing experimental approaches uses a low-pressure gaseous detector to measure individual ionisations of charged particle tracks in a macroscopic gas volume and to transfer the ionisation pattern to microscopic dimensions of water-equivalent density<sup>(5)</sup>. The scaling factor of  $10^{-5}$ – $10^{-6}$  is defined by the gas/water ratio of the mean free path length between ionisations. One of the detectors utilising this principle, the ion-counting nanodosimeter (ND), has been described by the authors in their previous work<sup>(6,7)</sup>. It registers and counts the number of positive ions induced per particle in an approximately cylindrical wall-less sensitive volume (SV)  $\sim 2$  mm diameter and 50 mm height, formed by electric fields within the central part of a much larger chamber (diameter 200 mm, height 50 mm) filled

with propane at 1.33 mbar (scaling factor  $3 \times 10^{-6}$ ). Using ion drift-time cuts, sub-segments of the SV can be selected (see Schemelinin *et al.* this issue).

Because the SV in the ion-counting ND is perfectly wall-less, nanodosimetric measurements cannot only be performed for particles crossing the SV but also for particles travelling at any distance from it, limited only by chamber walls. This simulates experimental conditions in radiobiology, where the distance of charged particle tracks from the DNA is random. Knowing the location of the primary particle path, one can probe the particle track structure with a nanometer-size equivalent volume. While this can be achieved using a highly collimated (sub-millimeter) particle beam, a more practical approach, realised in the present detector, is to employ a precision tracking system providing coordinate information on particle entrance and exit points in the chamber.

In this work, the performance of the ion-counting ND with tracking capabilities is described. Precise coordinate information on protons of 250 MeV crossing the SV combined with the ND data was used to determine the shape and efficiency map of the SV. Ion cluster size distributions were obtained as a function of distance from the particle track and compared to the results of a dedicated Monte Carlo track structure code.

\*Corresponding author: vbashkirov@dominion.llumc.edu

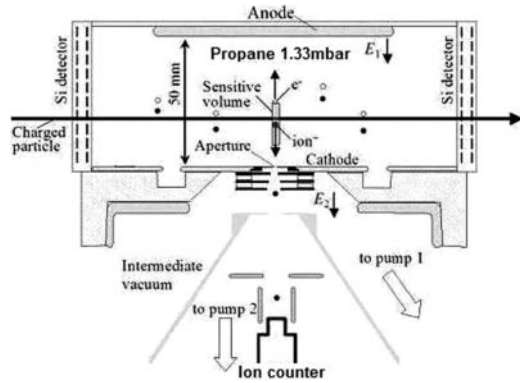


Figure 1. Cross section of the ion-counting ND with a schematic particle track producing electrons (open circles) and ions (closed circles).

## MATERIALS AND METHODS

### The ion-counting ND—design and principle of operation

Figure 1 shows the cross section of the ion-counting ND described in detail in Refs. (6,7). Its main components are a gas-filled ionisation chamber with an aperture at its bottom plate (cathode), ion focusing electrodes below the aperture, and a vacuum-operated ion counter. The ND detects positive ions, which are induced by protons (or other charged particles) within a small SV embedded in low-pressure gas (e.g. propane). The SV is shown in Figure 1 as an idealised shaded cylinder above the ND aperture. The actual shape and size of the SV in the gas is determined by the size of the aperture through which ions are extracted, the drift field  $E_1$  and the focusing field  $E_2$ . The homogeneous drift field  $E_1$  is defined by the voltage at the anode with respect to the cathode (ground). The ion-focusing and accelerating field  $E_2$  is defined by the voltages on electrodes below the ND aperture and on the first dynode of the ion counter. Two turbo-molecular pumps (not shown) generate the pressure gradient between the 1.33 mbar gas volume and the  $6.7 \times 10^{-5}$  mbar required for the ion counter operation (low noise electron multiplier SGE model AF180HIG)<sup>(6,7)</sup>.

### The tracking system

The ND at LLUMC is equipped with a silicon tracking telescope (STT). It consists of two silicon detector modules located at the entrance and exit of the gas volume.

Each vacuum-tight module (Figure 2) contains a pair of single-sided silicon strip detectors (SSDs) with their strips oriented at right angles. The SSDs are 400  $\mu\text{m}$  thick, have a pitch of 194  $\mu\text{m}$ , and a

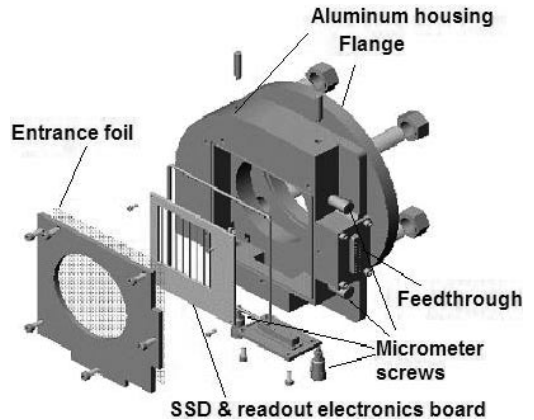


Figure 2. Exploded view of the STT module.

sensitive area of  $6.4 \times 6.4 \text{ cm}^2$ . The SSDs are fixed to opposite sides of a G10 frame board by gauge pins and bonded to the readout electronics located on the same board. Using four micrometer screws, the board orientation in the module is adjustable to permit accurate alignment of the detectors. The detector electronics is connected to the data acquisition (DAQ) system via a 25-pin vacuum-tight feedthrough. The electronics records the strip-hit number and particle specific energy deposition measured in each detector using the time-over-threshold technique. The detector electronics also generates a fast-OR signal of all strips. Coincidence of these signals from all four SSDs is used in the DAQ system as a primary particle trigger. A detailed description of the STT can be found elsewhere<sup>(8)</sup>.

### DAQ system

The original ND DAQ system<sup>(7)</sup> was modified to allow processing of the STT data. Modifications of the ND DAQ system included:

- (1) A custom repeater board, located on the ND side of the DAQ system, providing bi-directional command and data signals exchanged between PCI DAQ boards and the SSD modules. It also incorporates the STT trigger logic and low-noise STT power supplies.
- (2) A NI 6534 Digital Input/Output PCI board with a custom-built extension board to support readout of the STT data stream together with the ND ion signal pulse train in a common 100  $\mu\text{s}$  time window.

The DAQ software was written in Visual Basic and runs under Windows 2000 on a Pentium 4, 1.8 GHz PC. It provides the STT readout electronics programming and calibration, synchronised readout of the STT and the ND data, on-line data quality

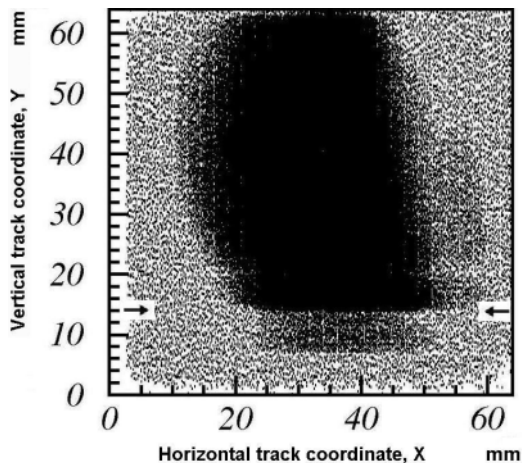


Figure 3. Distribution of reconstructed proton track positions in the central SV plane. Arrows show the aperture plate position.

control monitoring, and compression and storage to the PC hard drive. The data acquisition rate of the DAQ system is limited to  $<10$  K events  $s^{-1}$  by the 100  $\mu s$  per event readout window; the latter is dictated by the maximum ion drift time.

### Experimental setup and data taking

The measurements were performed on the p-east beam line located in the LLUMC Proton Treatment Center research room, where the ND is currently installed. The data were taken with a beam of 250 MeV protons shaped by the beam line magnet optics to a width of  $\sim 2$  cm and a height of 5 cm. The beam was centered on the SV under control of the on-line STT monitor. The beam profile in the SV plane as reconstructed by the STT is shown in Figure 3.

Data were taken each 2.2 s (accelerator cycle) at an average rate of 2000 events  $s^{-1}$  spill. The total dataset acquired in the experiment contained of the order of 70 million particle events. Initial data reduction included rejection of pile-up events, events with more than one track or incomplete tracks, events with abnormally large energy deposition in any of the SSDs, and events with track orientation inconsistent with the beam direction. After data reduction,  $\sim 40$  million events were available for further analysis.

### Monte Carlo simulation of the experiment

A Monte Carlo particle track structure code was used<sup>(7,9)</sup>. It utilises a compilation of experimental ionisation cross sections of protons and experimental electron interaction cross sections for elastic

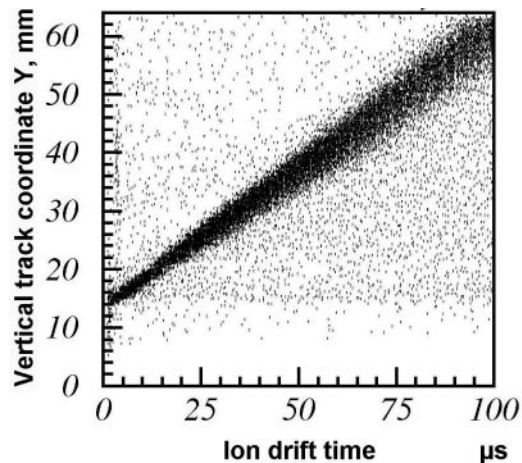


Figure 4. Correlation between measured ion drift time and vertical track coordinate.

scattering, excitation and ionisation to transport high-energy protons and secondary electrons with energies down to 10 eV in propane.

The ND layout was modelled in the code as an idealised, wall-less rectangular volume of  $5 \times 5 \times 3$   $cm^3$  filled with propane at 1.33 mbar simulating the gas volume surrounding the SV. The positions of the ions on a proton track segment in the gas volume were transformed into an ion-signal pulse train using a calculated efficiency 3-D map of the SV<sup>(6,7)</sup> and the experimentally measured ion space-drift time relationship (Figure 4). Noise of the ND ion channel was introduced into the pulse train as random pulses with a frequency corresponding to the measured one ( $\sim 5$  Hz). A number of  $10^8$  tracks were typically generated per Monte Carlo (MC) run.

## RESULTS

### Verification of the SV shape and efficiency

The collected data were used for verification of the previously calculated SV shape and efficiency distribution<sup>(6,7)</sup>. To this purpose, events with at least one registered ions were binned according to the reconstructed proton track coordinates in the central SV plane. In the resulting scatter plot (Figure 5), events are grouped in the expected SV shape, reflecting the SV ion collection efficiency map integrated along the primary particle tracks, i.e. along the Z-axis.

To make a quantitative comparison with the results of the MC simulation, the event distribution of Figure 5 was normalised to the experimental distribution of tracks (Figure 3). This resulted in the 2-D ( $X$ - $Y$ ) probability distribution to record one or more ions generated by protons crossing the SV.

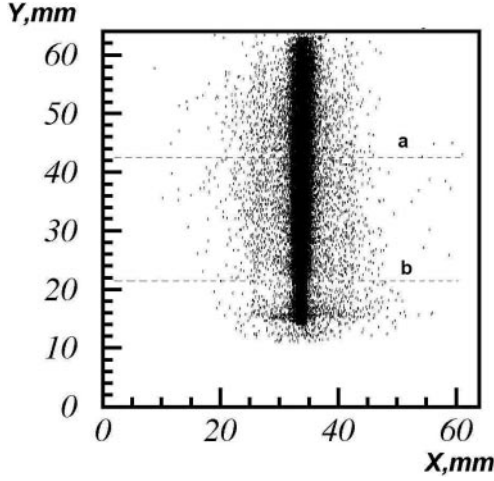


Figure 5. SV image; lines ‘a’ and ‘b’ show the position of slices presented in Figure 6a and b.

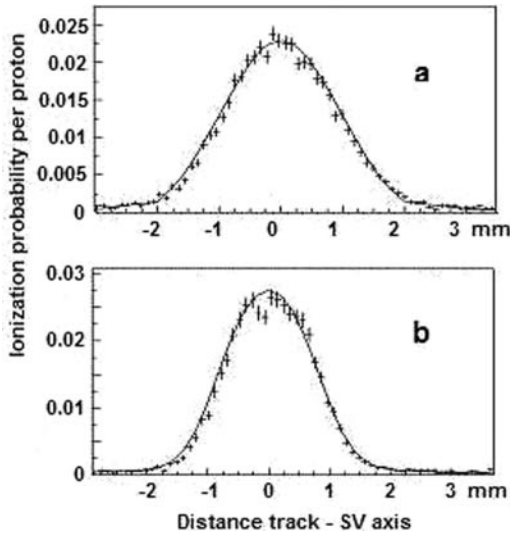


Figure 6. MC vs. experimental data. a:  $Y = 42.5$  mm, b:  $Y = 21.5$  mm.

In the corresponding MC-simulated distribution, a set of needle-like beams was used, traversing the ND gas volume at fixed  $X$  and  $Y$  coordinates corresponding to the experimental binning grid. For each grid point the probability of registering one or more ions was estimated as the ratio of the number of events with  $\geq 1$  ion to the total number of simulated events.

Figure 6 shows the resulting probability profiles for 1 mm SV slices at two  $Y$  levels (21.5 and 42.5 mm); the simulated probability (solid line) shows good agreement with the measured probability (error bars).

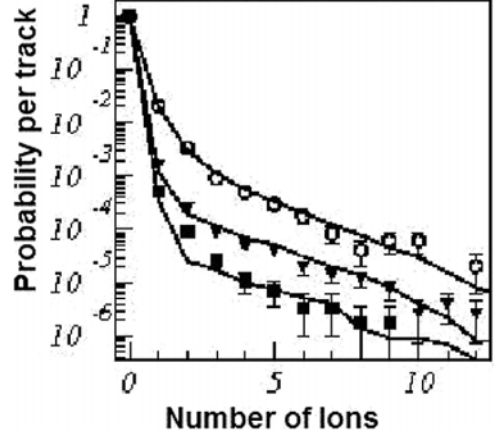


Figure 7. Ion cluster size distributions at 0 nm (open circles), 6 nm (inverted filled triangle) and 21 nm (filled square) distance from proton track. Solid lines are MC simulations.

### Ion cluster size distributions

The same experimental and simulated datasets were used to study the dependence of ion cluster size (ICS) distributions on the particle impact parameter (distance from the SV axis). Experimental ICS distributions were calculated for a set of impact parameters at  $Y = 29$  mm and compared to the ICS resulting from the MC simulation for the same beam coordinates. Examples of the resulting ICS distributions are presented in Figure 7 for impact parameters of 0, 6, and 21 nm.

Information on the spatial distribution of ions within the clusters, along the SV axis, can be retrieved from the measured ion arrival time distribution by utilising the space vs. drift time relationship shown in Figure 4. The precision of the ion position is determined by the spread of the ion arrival time, which increases with distance to aperture. Gaussian fitting of the arrival time distributions yielded an approximately linear dependence of the vertical coordinate resolution  $\sigma$  on the ion drift distance  $Y_d$ :

$$\sigma(\text{nm}) \approx 1.5 + 0.15 \times Y_d, \quad (1)$$

where  $Y_d$  is measured in mm. This means that the resolution of ion localisation is  $\sim 5$  nm at the center of the SV ( $Y_d = 25$  mm).

### CONCLUSION

An ion-counting ND with primary-particle tracking capabilities has been used to study the nanometric distribution of radiation-induced ions in low-pressure gases. The precision tracking capability allowed for verification of the ion registration

efficiency distribution within the SV possible, for which only a calculated map was available before. In experiments with a broad beam of 250 MeV protons, it was demonstrated that tracking information combined with nanodosimetric data allows characterisation of ionisation pattern produced by charged particles both crossing the SV and passing at arbitrary distance from it. Measurable quantities include the number of ions per cluster and their coordinate along the SV axis with a resolution of  $\sim 5$  tissue-equivalent nanometers. Tracking ion-counting nanodosimetry allows measuring these quantities as a function of primary-particle impact parameter. Experimental data and data simulated by a dedicated Monte Carlo track structure code were found to be in good agreement, which supports the application of the ion-counting technique in experimental track-structure studies.

#### ACKNOWLEDGEMENTS

This work was partially supported by the US National Medical Technology Testbed Inc. (NMTB) under the US Department of the Army Medical Research Acquisition Activity, Cooperative Agreement Number DAMD17-97-2-7016 and by the German Minerva Foundation. A.B. is the W.P. Reuther Professor of research in the peaceful use of atomic energy.

#### REFERENCES

1. Ward, J. F. and Ward, J. F. *DNA damage produced by ionizing radiation in mammalian cells: identities, mechanisms of formation and reparability*. Prog. Nucleic Acid Res. Mol. Biol. **35**, 95–125 (1988).
2. Schulte, R. W. M. *Prediction of cellular effects of high and low-LET irradiation based on the energy deposition pattern at the nanometer level*. In: Microdosimetry. An Interdisciplinary Approach. Goodhead, D. T., O'Neill, P. and Menzel, H., Eds. (Cambridge: Royal Society of Chemistry) pp. 211–214 (1997).
3. Nikjoo, H., Uehara, S., Wilson, W. E., Hoshi, M. and Goodhead, D. T. *Track structure in radiation biology: theory and applications*. Int. J. Radiat. Biol. **73**, 355–364 (1998).
4. Geant 4 DNA project. Available on <http://www.ge.infn.it/geant4/dna/>
5. Schuhmacher, H. and Dangendorf, V. *Experimental tools for track structure investigations: new approaches for dosimetry and microdosimetry*. Radiat. Prot. Dosimetry **99**, 317–323 (2002).
6. Garty, G., Shchemelinin, S., Breskin, A., Chechik, R., Orion, I., Guedes, G. P., Schulte, R., Bashkirov, V. and Grosswendt, B. *Wall-less ion-counting nanodosimetry applied to protons*. Radiat. Prot. Dosimetry **99**, 325–330 (2002).
7. Garty, G., Shchemelinin, S., Breskin, A., Chechik, R., Assaf, G., Orion, I., Bashkirov, V., Schulte, R. and Grosswendt, B. *The performance of a novel ion-counting nanodosimeter*. Nucl. Instrum. Meth. A **491**, 212–235 (2002).
8. Keeney, B., Bashkirov, V., Johnson, R. P., Kroeger, W., Oyama, H., Sadrozinski, H. F., Schulte, R. W. M., Seiden, A. and Spradlin, P. *A silicon telescope for applications in nanodosimetry*. IEEE Trans. Nucl. Sci. **49**, 1724–1727 (2002).
9. Grosswendt, B., de Nardo, L., Colautti, P., Pszona, S., Conte, V. and Tornielli, G. *Experimental equivalent cluster-size distributions in nanometric volumes of liquid water*. Radiat. Prot. Dosim. **110**, 851–857 (2004).